

Electrodeposition of lead alloys from fluoborate baths

R. FRATESI, G. ROVENTI

Istituto di Scienza dei Materiali, Facoltà di Ingegneria, Università di Ancona, Italy

M. MAJA, N. PENAZZI

Sezione di Elettrochimica e Corrosione del Dipartimento di Scienza dei Materiali ed Ingegneria Chimica, Politecnico di Torino, Italy

Received 22 September 1983; revised 31 October 1983

The codeposition of some elements with lead from fluoborate baths has been studied in order to obtain lead alloys with a low concentration of a second metal. The metals considered were As, Bi, Cu, Sb, Se, Sn and Te. The chemical analysis of alloys obtained in various electrolysis conditions permitted an investigation of the kinetic behaviour of the metals codeposited with lead. The results showed that only Bi, Sb, Se and Te attain a limiting value of discharge current density and that the codeposition is regular for all metals. SEM observation of the deposits revealed that Sb and Se have a marked influence on the crystal morphology while the remaining metals induce only minor modifications.

1. Introduction

Various electrodeposited lead alloys have been studied in the past [1-4] because of their promising capability for resistance to corrosion and wear. DuRose and Blum [5] have pointed out that electroplated coatings show structural and mechanical properties that make them preferable in various cases to the more readily applicable hot dipped coatings.

More recently, electrodeposited lead alloys have found industrial application in the production of etch-resistant coatings and enhanced solderability coatings.

Lead-tin alloys are actually the most frequently used among electrodeposited lead alloys. By varying the tin content from 40 to 60% these alloys can suit all the applications mentioned above. Lead-antimony, lead-copper, lead-bismuth, lead-thallium and lead-silver electrodeposited alloys are valuable for their corrosion protection and wear resistance properties. They have been extensively investigated, yet there are still problems in reaching the full practicability of the process. The same situation applies to the electrodeposition of ternary alloys lead-tin-copper, lead-antimony-copper and lead-antimony-tin that seem to provide coatings of

better quality than pure lead and lead-tin and that need easier to operate electrodeposition baths.

Besides the fields of industrial usage previously considered, research on low-content lead alloy electrodeposition is also important in lead electrorefining and in the process of electrochemical recovery of lead from spent batteries [6]. It is, in fact, important in these processes to have a full knowledge of the behaviour of the impurities present in the bath, in order to obtain high purity lead or to recover, directly from spent batteries, alloys suitable for battery grid manufacture.

Bearing in mind this aspect of the more general subject of lead alloy electrodeposition, we have investigated and compared the behaviour of As, Bi, Cu, Sb, Se, Sn and Te codeposited with lead.

As the fluoborate bath is widely used in the industrial electrodeposition of lead and its alloys, because of the higher deposition current densities, all the alloys examined in the present work have been deposited from this kind of solution.

For some of the elements considered many valuable studies have been made previously, but literature has been found lacking for lead-arsenic, lead-selenium and lead-tellurium alloys.

The cathodic deposits, obtained in different electrolysis conditions, have been analysed to determine the amount of metal codeposited with

lead; from these data the partial polarization curves of the various metals have been traced. The surface morphology of the deposits has also been investigated by means of scanning electron microscopy (SEM).

2. Experimental details

The deposition has been carried out, at constant current, in a polyethylene cell. The working electrode, having a 2 cm^2 surface area, was a pure graphite cylinder embedded in acrylic resin. The counter-electrode was a platinum foil and the reference a mercurous sulphate electrode connected to the cell by means of K_2SO_4 in an agar-agar salt bridge.

Before every test the electrode surface was polished with 800 grade emery paper. All the solutions were prepared using doubly distilled water and analytical grade reagents. Lead was added to the fluoboric acid solutions as lead oxide and the alloying metals as oxides or nitrates.

The electrodeposition baths contained 50 g l^{-1} of Pb^{2+} , 42 g l^{-1} of fluoboric acid and various quantities of the alloying metals: from 10 to 200 mg l^{-1} of As^{3+} , Bi^{3+} , Se^{4+} and Te^{4+} and from 10 to 1000 mg l^{-1} of Cu^{2+} , Sn^{2+} and Sb^{3+} . Only one metal, apart from lead, was present in each bath.

Electrodeposition was performed at various current densities, from 5 to 40 mA cm^{-2} , and compact and coherent deposits were obtained throughout the range of current density by means of additions of peptone, an organic additive known for its levelling properties. We have found that in most cases peptone exerted a negligible influence on the partial current density values. In the case of arsenic only did this additive significantly lower the quantity of metal codeposited, as can be seen from Figs. 4 and 5 in Section 3.

During the tests, carried out at 25°C without stirring the solution, the cathodic potential was recorded. After 1 h of electrodeposition the deposit was detached from the electrode, washed in doubly distilled water, in alcohol and dried. It was then weighed, dissolved in HNO_3 1:1 solution and analysed by means of the ICP spectroscopic technique (Perkin-Elmer 5005 model).

In the first experiments performed the H_2 volume evolved during electrolysis was also measured but this procedure was ceased because

the values of the partial hydrogen current obtained were negligible.

All the tests were repeated at least three times and gave good agreement of the data.

Observation by means of the scanning electron microscope was also carried out on parts of the deposits used for the chemical analysis, in order to examine the surface morphology of the various alloys.

3. Results and discussion

3.1. Kinetics of alloy electrodeposition

From the chemical analysis of the deposits, obtained under various experimental conditions, partial polarization curves $i(V)$ were traced for lead and the metals considered. These curves, some of which are reported in Figs. 1 and 2, show that bismuth, antimony, selenium and tellurium attain a limiting value of the discharge current density in the potential range of lead deposition. No such limiting value can be found in the case of arsenic, copper and tin.

It must be noted also that tellurium discharges

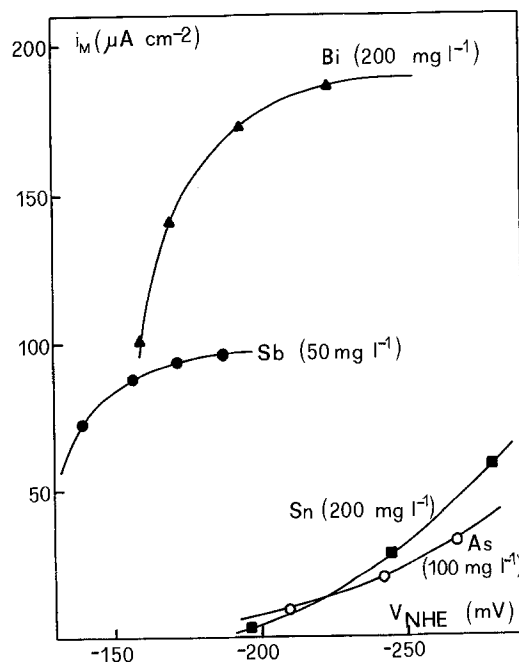


Fig. 1. Partial polarization curves for As, Bi, Sb and Sn. Electrolysis conditions: 42 g l^{-1} HBF_4 ; 30 g l^{-1} H_3BO_3 ; 50 g l^{-1} Pb^{2+} ; 0.2 g l^{-1} (2 g l^{-1} for Sn) peptone; 25°C .

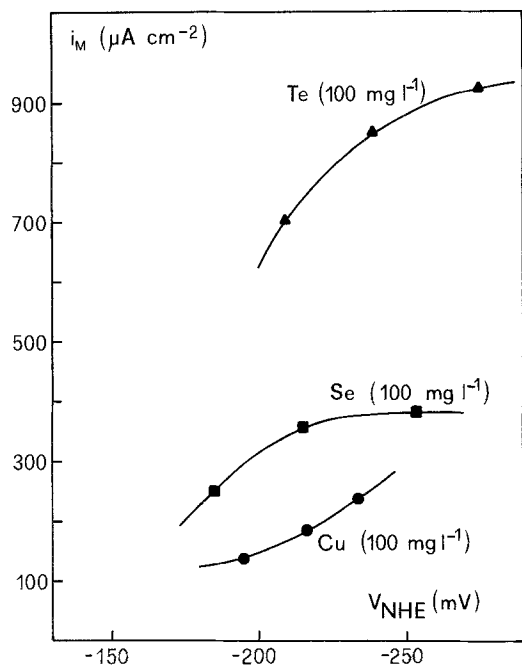


Fig. 2. Partial polarization curves for Cu, Se and Te. Electrolysis conditions: $42 \text{ g l}^{-1} \text{ HBF}_4$; $30 \text{ g l}^{-1} \text{ H}_3\text{BO}_3$; $50 \text{ g l}^{-1} \text{ Pb}^{2+}$; 0.2 g l^{-1} peptone; 25° C .

at current densities which appear abnormally high if compared with the corresponding values of the other metals, in particular, selenium.

In order to assist discussion of the experimental data, polarographic analyses of the metals in fluoborate solution have been carried out leading to the determination of the corresponding diffusion coefficients in Table 1. No result was obtained in the case of tin because of the impossibility of detecting any polarographic wave in the conditions chosen. Moreover, the diffusion coefficient for tellurium must be taken with some caution because of the known difficulties [7] in the interpretation of Te^{4+} polarograms.

Table 1. Values of the diffusion coefficient, D , and the diffusion layer thickness, δ , for the metals examined.

Metal	$D (10^{-6} \text{ cm}^2 \text{ s}^{-1})$	$\delta (10^{-2} \text{ cm})$
arsenic	7.0	—
bismuth	5.9	0.9
copper	7.5	—
antimony	8.4	1.0
selenium	7.4	0.8
tellurium	0.8	0.03

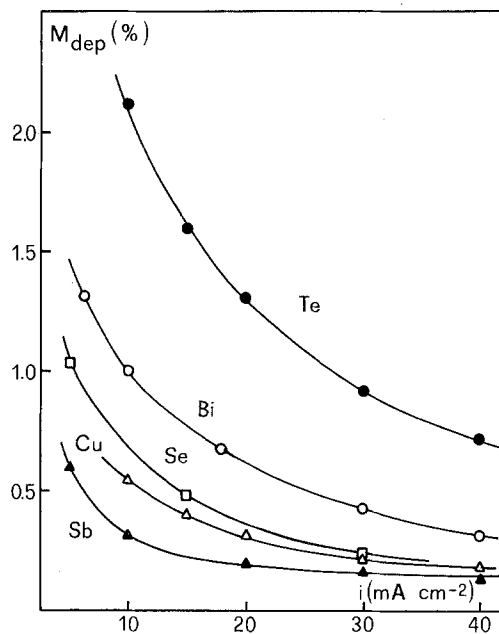


Fig. 3. Metal percentage in the deposit M_{dep} vs the total electrolysis current density, i . Electrodeposition conditions: $200 \text{ mg l}^{-1} \text{ Bi}^{3+}$; $50 \text{ mg l}^{-1} \text{ Sb}^{3+}$; $100 \text{ mg l}^{-1} \text{ Cu}^{2+}$, Se^{4+} and Te^{4+} ; $42 \text{ g l}^{-1} \text{ HBF}_4$; $30 \text{ g l}^{-1} \text{ H}_3\text{BO}_3$; $50 \text{ g l}^{-1} \text{ Pb}^{2+}$; 0.2 g l^{-1} peptone; 25° C .

From Fick's diffusion law it has been possible to calculate the diffusion layer thickness, δ , of the metals whose limiting current density could be determined.

The δ values, reported in Table 1 with the exception of tellurium, range around 0.01 cm and are consistent with the results reported in literature [1, 8, 9]. The low δ value found for tellurium is related to the uncertainty in the diffusion coefficient determination and to its peculiarly high partial current densities. These values, calculated from the tellurium content in the alloys, would not be so anomalous if Te^{2+} ions were supposed to be present in the bath instead of Te^{4+} ions. No evidence supporting this suggestion, however, has been found.

In the case of arsenic, copper and tin* the limiting current densities, calculated using as δ the mean of bismuth, antimony and selenium values, came out to be in all cases higher than the

* For tin a diffusion coefficient of $7.2 \times 10^6 \text{ cm}^2 \text{ s}^{-1}$ has been assumed, the mean of the values of Bi, As, Cu, Sb and Se.

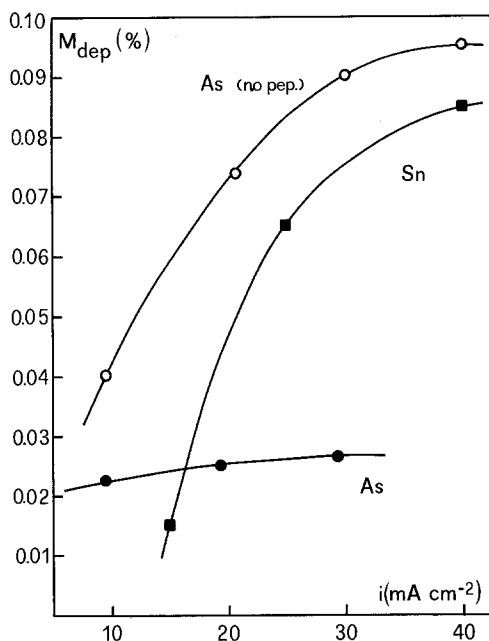


Fig. 4. Metal percentage in the deposit, M_{dep} vs the total electrolysis current density, i . Electrodeposition conditions: $100 \text{ mg l}^{-1} \text{ As}^{3+}$; $200 \text{ mg l}^{-1} \text{ Sn}^{2+}$; $42 \text{ g l}^{-1} \text{ HBF}_4$; $30 \text{ g l}^{-1} \text{ H}_3\text{BO}_3$; $50 \text{ g l}^{-1} \text{ Pb}^{2+}$; peptone: 0.2 and 0 g l^{-1} for As, 2 g l^{-1} for Sn; 25° C .

experimental data. The conclusion from this finding is that these metals can also codeposit under diffusion control, as confirmed for tin and copper by many authors [1, 5]. They reach the limiting value of discharge current density at potentials higher than those obtained in our tests.

The variation of the metal content in the alloys with increase of the total electrolysis current density is shown by the curves of Figs. 3 and 4. The trend is characteristic of metals codepositing with lead under diffusion control as more noble (Fig. 3) and less noble metals (Fig. 4). As previously observed, the influence of peptone on arsenic codeposition is quite evident.

For those metals whose percentage in the deposit decreases as the current rises (Fig. 4) we have derived an empirical relation involving the metal content in the deposit, that in the bath and the electrolysis current density. This expression, similar to those obtained by other authors [10–13], does not have a general validity but holds true in the particular conditions of our tests. The formula is as follows:

Table 2. K and K' values for Expression 1. They are valid for: $T = 25^\circ \text{ C}$; $0.01 (\text{A cm}^{-2}) < i < 0.04 (\text{A cm}^{-2})$.

Metal	$K (\text{A cm g}^{-1})$	$K' (\text{cm}^3 \text{ g}^{-1})$
bismuth	50.8	0.38
copper	45.0	0.95
antimony	52.1	0.80
selenium	58.5	0.70
tellurium	194.0	2.15

$$M_{\text{dep}} = \frac{K + (K' i \times 10^3)}{i} [M] \quad (1)$$

where M_{dep} is the percentage of the metal, M , in the alloy, $[M]$ is the concentration of M in the bath in g cm^{-3} , i is the total electrolysis current density in A cm^{-2} , K and K' are constants for the metal considered and are reported in Table 2.

It is important to note that the behaviour of bismuth, antimony and selenium is well described by similar values of K and K' and that the same is

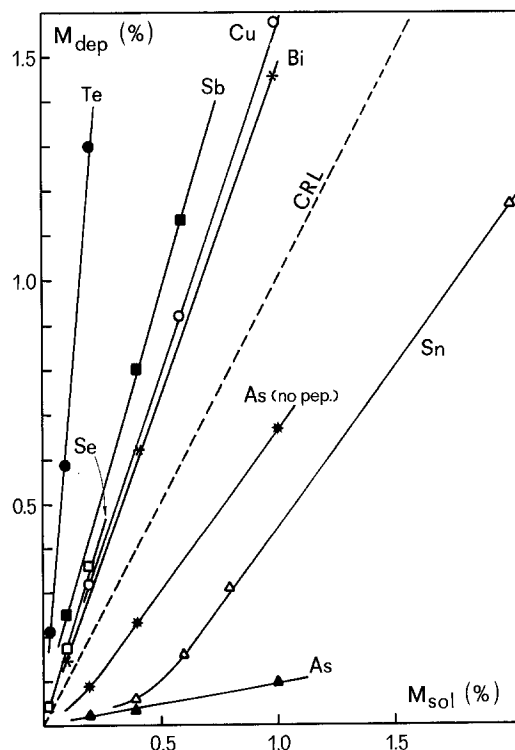


Fig. 5. Plot of the metal percentage in the deposit, M_{dep} vs the metal percentage in the solution M_{sol} . Electrolysis conditions: 20 mA cm^{-2} total current density; $42 \text{ g l}^{-1} \text{ HBF}_4$; $30 \text{ g l}^{-1} \text{ H}_3\text{BO}_3$; $50 \text{ g l}^{-1} \text{ Pb}^{2+}$; 0.2 g l^{-1} peptone (0.2 and 0 g l^{-1} for As, 2 g l^{-1} for Sn); 25° C .

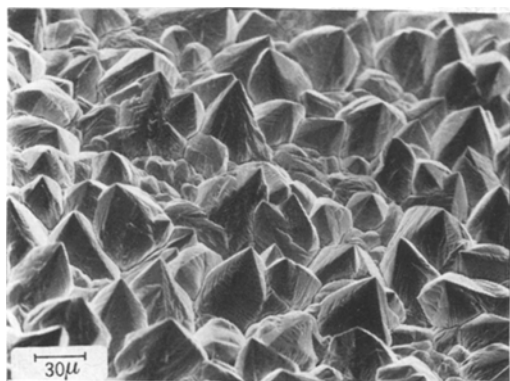


Fig. 6. Pure lead electrodeposited at 15 mA cm^{-2} from a bath containing: $42 \text{ g l}^{-1} \text{ HBF}_4$; $30 \text{ g l}^{-1} \text{ H}_3\text{BO}_3$; $50 \text{ g l}^{-1} \text{ Pb}^{2+}$; 0.2 g l^{-1} peptone. $T = 25^\circ \text{ C}$.

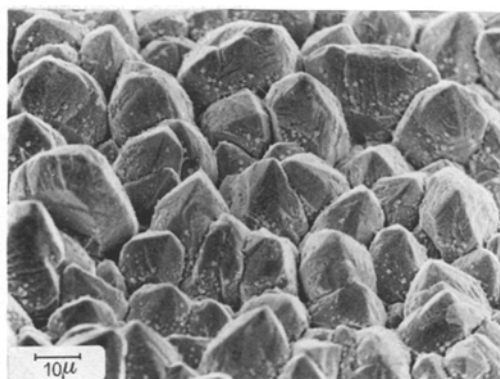


Fig. 8. Electrodeposited lead-copper alloy. Electrolysis conditions: $100 \text{ mg l}^{-1} \text{ Cu}^{2+}$; $42 \text{ g l}^{-1} \text{ HBF}_4$; $30 \text{ g l}^{-1} \text{ H}_3\text{BO}_3$; $50 \text{ g l}^{-1} \text{ Pb}^{2+}$; 0.2 g l^{-1} peptone; 30 mA cm^{-2} total current density; 25° C .

true also for copper. K and K' for tellurium are, on the contrary, quite high so highlighting the anomalous behaviour of this element.

Fig. 5 shows a plot of the percentage of the metal in the alloy against the one in the bath, for all metals considered. It can easily be seen that the metals found to be more noble than lead (Fig. 3) exhibit curves lying above the composition reference line, rapidly rising from the origin and are therefore preferentially deposited. The opposite happens for arsenic and tin which codeposit with lead as the less noble metal.

All the results obtained indicate that the electrodeposition of the lead alloys considered is regular according to the classification made by Brenner [1], i.e. these metals discharge with lead under diffusion control.

3.2. Morphology of the deposits

Observation of the deposits with the scanning electron microscope confirmed that the surface was in all cases compact and the deposit coherent. Fig. 6 illustrates the morphology of a pure lead deposit where regular, pyramid-like growths can be seen. As the electrodeposition current density rises, the size of the grains increases making the 'pyramids' more pronounced.

The metals codeposited with lead exert a certain influence on the deposit morphology, modifying it drastically in some cases. Arsenic, bismuth, copper, tin and tellurium maintain the gross structure of the pure lead deposits with some minor modifications (Figs. 7 and 8). An increase in the amount of the alloying metal causes an

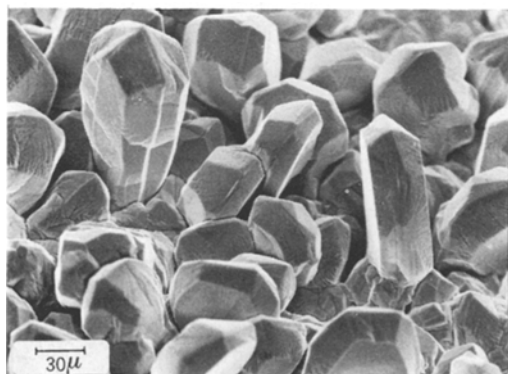


Fig. 7. Electrodeposited lead-bismuth alloy. Electrolysis conditions: $50 \text{ mg l}^{-1} \text{ Bi}^{3+}$; $42 \text{ g l}^{-1} \text{ HBF}_4$; $30 \text{ g l}^{-1} \text{ H}_3\text{BO}_3$; $50 \text{ g l}^{-1} \text{ Pb}^{2+}$; 0.2 g l^{-1} peptone; 30 mA cm^{-2} total current density; 25° C .

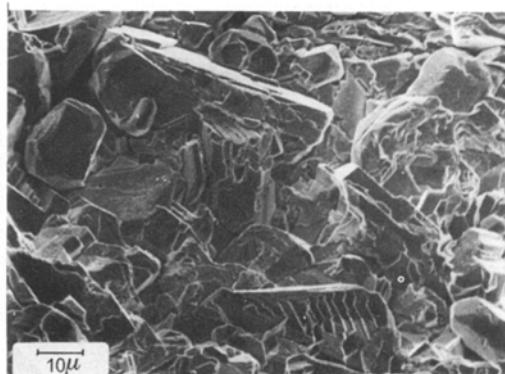


Fig. 9. Electrodeposited lead-antimony alloy. Electrolysis conditions: $50 \text{ mg l}^{-1} \text{ Sb}^{3+}$; $42 \text{ g l}^{-1} \text{ HBF}_4$; $30 \text{ g l}^{-1} \text{ H}_3\text{BO}_3$; $50 \text{ g l}^{-1} \text{ Pb}^{2+}$; 0.2 g l^{-1} peptone; 5 mA cm^{-2} total current density; 25° C .

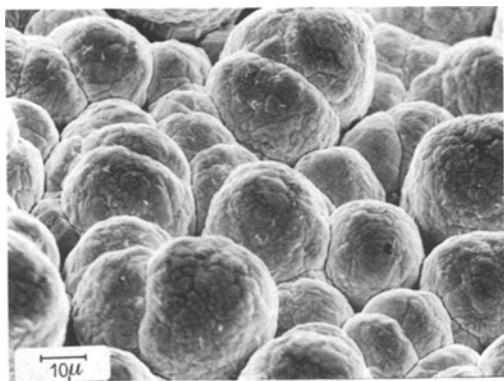


Fig. 10. Electrodeposited lead-selenium alloy. Electrolysis conditions: $50 \text{ mg l}^{-1} \text{ Se}^{4+}$; $42 \text{ g l}^{-1} \text{ HBF}_4$; $30 \text{ g l}^{-1} \text{ H}_3\text{BO}_3$; $50 \text{ g l}^{-1} \text{ Pb}^{2+}$; 0.2 g l^{-1} peptone; 30 mA cm^{-2} total current density; 25° C .

enlargement of the grains and an increase in the deposition current exerts the same effect as in pure lead deposits.

More noticeable modifications of the morphology takes place in the case of lead-antimony and lead-selenium alloys. The deposit of Fig. 9 shows a completely different morphology: the grains are finer with an irregular shape. Grain refinement is more evident as the antimony concentration in the bath increases while a higher electrolysis current density, causing the depletion of the antimony content in the deposit, has the opposite effect.

Lead-selenium alloys show a completely different morphology, Fig. 10. The boulders appearing

at the surface increase slightly in size as the selenium content in the deposit is increased.

Acknowledgement

Financial support of this work by the Consiglio Nazionale delle Ricerche (CNR, Rome) is gratefully acknowledged.

References

- [1] A. Brenner, 'Electrodeposition of Alloys' Vols. I and II, Academic Press, New York (1963).
- [2] R. Walker, *Metal Finish J.* **18** (1972) 334.
- [3] *Idem*, *Int. Metal. Rev.* **19** (1974) 1.
- [4] J. A. von Fraunhofer, 'The Electrochemistry of Lead', edited by A. T. Kuhn, Academic Press, New York (1979) Ch. 6.
- [5] A. H. DuRose and W. Blum, 'Modern Electroplating', edited by F. A. Lowenheim, Wiley, New York (1967) Ch. 11.
- [6] M. V. Ginatta, West German Patent No. 2 527 434 (1976) and US Patent No. 4 098 658.
- [7] S. I. Zhdanov, 'Encyclopedia of the Electrochemistry of the Elements', edited by A. J. Bard, Vol. IV, M. Dekker Inc., New York (1975) p. 404.
- [8] K. J. Vetter, 'Electrochemical Kinetics. Theoretical and Experimental Aspects', Academic Press, New York (1967) p. 188.
- [9] J. O'M. Bockris, 'Modern Electrochemistry', Vol. II, Plenum Press, New York (1970) p. 1055.
- [10] E. D. Kochman, G. A. Krinari and V. N. Gusev, *Prot. Met.* **14** (1978) 176.
- [11] *Idem*, *ibid.* **13** (1977) 295.
- [12] K. M. Tyutina, N. T. Kudryavtsev, G. A. Selivanova and A. N. Popov, *ibid.* **14** (1978) 516.
- [13] V. V. Bogoslovskii, K. M. Tyutina and N. T. Kudryavtsev, *ibid.* **11** (1975) 468.